A Novel Linear, Unbiased Estimator to Fuse Delayed Measurements in Distributed Sensor Networks with Application to UAV Fleet

Ronan Arraes Jardim Chagas[1] and Jacques Waldmann[2]

***Abstract*— This paper proposes a novel methodology to fuse delayed measurements in a distributed sensor network. The algorithm derives from the linear minimum mean square error estimator and yields a linear, unbiased estimator that fuses the delayed measurements. Its performance regarding the estimation accuracy, computational workload and memory storage needs is compared to the classical Kalman filter reiteration that achieves the minimum mean square error in linear and Gaussian systems. The comparison is carried out using a simulated distributed sensor network that consists of a UAV fleet in formation flight in which the GPS measurements and relative positions are exchanged among neighboring network nodes. The novel technique yields similar performance to the reiterated Kalman filtering, which is the optimal linear Gaussian solution, while demanding less storage capacity and computational throughput in the problems of interest.**

I. INTRODUCTION

A network consisting of spatially distributed sensor nodes with local processing units for acquiring local measurements and estimating the state vector of a dynamic system can produce more accurate estimates when information is exchanged among the nodes. Such distributed estimation approach is less susceptible to a single point failure that can cripple centralized estimation schemes [1], [2].

The processing unit at each sensing node iterates a Kalman filter. Two distinct possibilities were evaluated in literature: exchanging sensor measurements among nodes [3], [4], [5] and exchanging state vector estimates produced by the local Kalman filters [1], [2].

Distributed filtering has been widely investigated when network nodes share the dynamic model [1], [2], [3], [4]. However, interesting problems call for algorithms that can perform the distributed estimation when the nodes do not share the state-model, e.g. an UAV fleet [6], a set of satellites in orbit [7], [8], and spacecrafts flying into the deep space [9], [10], [11]. To the best knowledge of the authors, the first approach to information fusion in such a network was [12]. A very similar algorithm was proposed in [13]. In both investigations the nodes' states should be related by a linear transformation. Here, the subject is probed further to deal with delayed measurements in a distributed network wherein a particular dynamic model is embedded in each node. It is shown here that in such a scenario the exchanged measurements can only be fused if additional information is gathered to relate measurements from neighboring nodes with a node's state.

It is expected that the required information will arrive with delays. The accuracy of the distributed estimation by the network could be severely degraded had the delayed measurements been processed without adequate caution. There are a myriad of techniques in the literature to fuse delayed measurements in a non-distributed estimation. [14] compared many methods regarding performance, storage necessity, and computational workload. Among the techniques discussed, [15], [16], [17] need the knowledge that a delayed measurement has not been received at a node so that parallel computations can be started to optimally fuse the delayed measurement when it arrives. On the other hand, the algorithms in [18], [19] have not been extended to handle multiple delays. These inconveniences preclude the use of such algorithms in distributed estimation problems. [20] compared algorithms to fuse out-of-sequence measurements in sensor networks, which can be used in the distributed filtering problem addressed here. These algorithms were developed to achieve the minimum mean square error (MMSE) optimality in linear and Gaussian systems and thus require recursions that yield a heavy computational burden.

In the problems of interest, it is expected that measurements may be received with a delay on the order of thousands of the sampling step. Thus, algorithms that call for recursions will be time consuming. Here, a novel approach, thereafter called measurement transportation, has been developed based on the delayed-state Kalman filter [21] and on the suboptimal technique in [22]. This novel algorithm has been compared with a classical methodology for delayed measurement fusion: the reiterated Kalman filter [23]. This technique assures MMSE optimality if the system is linear and Gaussian.

A simulated UAV fleet in formation flight is the sensor network scenario in which GPS measurements and relative positions are exchanged among the aircraft. It turns out that this novel technique needs less storage capacity than any algorithm in [20], the computational workload is lighter in comparison with the reiterated Kalman filter, and a good overall performance is achieved for the problems of interest.

Sections II and III present coordinate frames and a glossary of acronyms, respectively. The distributed estimation problem when the nodes do not share the same state dynamics model is presented in section IV. The two algorithms to fuse the delayed measurements are described in section V.

*This work was financially supported by the project FINEP/CTA/INPE SIA (Inertial Systems for Aerospace Application, in Portuguese)

[1]Ronan Arraes Jardim Chagas is a Ph.D. student at Instituto Tecnológico de Aeronáutica (Technological Institute of Aeronautics), Division of Electronics Engineering, 12.228-900 SP São José dos Campos, Brazil `ronan.jardim at gmail.com`

[2]Jacques Waldmann is an Associate Professor at Instituto Tecnológico de Aeronáutica (Technological Institute of Aeronautics), Division of Electronics Engineering, 12.228-900 SP São José dos Campos, Brazil `jacques at ita.br`

The distributed filtering in a UAV fleet is described in section VI. Simulations and results are presented in section VII. Finally, the conclusions are written in section VIII.

II. Coordinate frames

The **true local horizontal frame** is used to represent the INS errors. In the true vehicle position, its X-axis points towards north, its Y-axis points towards east, and its Z-axis points down. This coordinate system is thereafter indicated with the l subscript.

The **computed coordinate frame** is defined as the local horizontal frame at the position computed by the INS.

The **platform coordinate frame** is defined as the local horizontal frame computed by the INS.

The **body coordinate frame** is defined as the inertial sensors coordinate frame. It is usually assumed to be aligned with the vehicle coordinate frame in strapdown IMUs or aligned with the platform coordinate frame in IMUs mounted on a stabilized platform. This coordinate frame is thereafter indicated with the b subscript.

The **Earth-Centered-Earth-Fixed** coordinate frame has its origin at the center of the Earth, its X axis lies on the equatorial plane and points to the Greenwich meridian, its Z axis is aligned with the Earth's rotation axis, and its Y axis completes the right-hand coordinate frame. It is thereafter indicated with the e subscript.

The **WGS-84 ellipsoid Earth-fixed coordinate frame** is used to represent the GPS data.

III. Notation and Abbreviations

DCM	Direction Cossine Matrix
MMSE	Minimum Mean Square Error
y	Scalar
$\mathbf{y}$	Vector
$\mathbf{A}$	Matrix
$\mathbf{I}_n$	Identity matrix of size n.
$[\mathbf{y}]_\times \mathbf{x}$	Matrix representation of the cross product $\mathbf{y} \times \mathbf{x}$.
$\mathbf{D}_b^a$	DCM that rotates from the a coordinate frame to the b coordinate frame.
$\boldsymbol{\rho}_l$	Transport rate represented in the local horizontal frame.
$\boldsymbol{\Omega}_{e,l}$	Earth's angular rate represented in the local horizontal frame.
$\mathbf{Asp}_l$	Specific force represented in the local horizontal frame.
$\boldsymbol{\Delta}\mathbf{R}_l$	INS position error represented in the local horizontal frame.
$\boldsymbol{\Delta}\mathbf{V}_l$	INS velocity error represented in the local horizontal frame.
$\boldsymbol{\Psi}$	Misalignment from the computed coordinate frame to the platform coordinate frame.
$\boldsymbol{\nabla}$	Accelerometer triad bias.
$\boldsymbol{\epsilon}$	Rate-gyro triad drift.
R_e	Earth radius at the latitude of the vehicle.
g_e	Gravitation at the latitude of the vehicle.
$\boldsymbol{\Omega}_{k-1,i}$	Set of all measurements received by the i-th node up to instant $k-1$.
$\hat{\mathbf{x}}_{k\|k-1,i}$	Estimate of the vector $\mathbf{x}_{k,i}$ using all measurement up to instant $k-1$.
$\mathbf{P}_{k\|k-1,i}$	Estimation error covariance of the vector $\mathbf{x}_{k,i}$ using all measurement up to instant $k-1$.

IV. Distributed Estimation

Distributed estimation has been widely studied in the literature using a set of sensors that measure states components from a common process dynamics [1], [2], [3], [4]. Many algorithms have been developed to fuse the network data to improve the overall estimation accuracy and to provide robustness. The exchanged information can be the state vector estimates from the neighboring nodes or the measurements from the corresponding sensors. However, many interesting problems call for algorithms that can perform distributed estimation when each node observes a different process, e.g. an UAV fleet. This scenario is modeled as follows for the i-th node:

$$\begin{aligned} \mathbf{x}_{k+1,i} &= \mathbf{F}_{k,i}\mathbf{x}_{k,i} + \mathbf{B}_{k,i}\mathbf{u}_{k,i} + \mathbf{G}_{k,i}\mathbf{w}_{k,i} \\ \mathbf{y}_{k,i} &= \mathbf{H}_{k,i}\mathbf{x}_{k,i} + \mathbf{v}_{k,i} \end{aligned} \tag{1}$$

where $\mathbf{F}_{k,i}$ is a $M_i \times M_i$ state-transition matrix, $\mathbf{B}_{k,i}\mathbf{u}_{k,i}$ is a deterministic and known control vector, $\mathbf{G}_{k,i}\mathbf{w}_{k,i}$ is the model noise assumed to be a zero-mean, white Gaussian random vector with $\mathbf{Q}_{k,i}$ covariance matrix, $\mathbf{H}_{k,i}$ is a $N_i \times M_i$ measurement matrix, and $\mathbf{v}_{k,i}$ is the measurement noise modeled as a zero-mean, white Gaussian random vector with $\mathbf{R}_{k,i}$ covariance matrix. The initial state $\mathbf{x}_{0,i}$ is a Gaussian random vector with mean $\mathbf{m}_{0,i}$ and covariance $\mathbf{P}_{0,i}$. Additionally it is assumed that all measurement and model noises through the network are independent to each other and are also independent to the initial state $\mathbf{x}_{0,i}$ at every node.

As mentioned before, the nodes does not share the same dynamics, thus the j-th node measurement cannot be directly used by the i-th node. If the latter receives, in the instant k, a measurement from the former, then the posterior probability density function is:

$$p(\mathbf{x}_{k,i}|\mathbf{y}_{k,i}, \mathbf{y}_{k,j}, \boldsymbol{\Omega}_{k-1,i}) \tag{2}$$

where $\boldsymbol{\Omega}_{k-1,i}$ is the set of all fused measurements up to instant $k-1$ at node i. Using Bayes rules, one can verify that:

$$\begin{aligned} &p(\mathbf{x}_{k,i}|\mathbf{y}_{k,i}, \mathbf{y}_{k,j}, \boldsymbol{\Omega}_{k-1,i}) = \\ &= C_k p(\mathbf{y}_{k,j}|\mathbf{x}_{k,i}, \mathbf{y}_{k,i}, \boldsymbol{\Omega}_{k-1,i}) p(\mathbf{y}_{k,i}|\mathbf{x}_{k,i}) p(\mathbf{x}_{k,i}|\boldsymbol{\Omega}_{k-1,i}) \end{aligned} \tag{3}$$

with C_k being a normalizing constant that yields to $\int_{\mathbb{R}^{M_i}} p(\mathbf{x}_{k,i}|\mathbf{y}_{k,i}, \mathbf{y}_{k,j}, \boldsymbol{\Omega}_{k-1,i}) d\mathbf{x}_{k,i} = 1$.

The computation of the p.d.f. $p(\mathbf{y}_{k,j}|\mathbf{x}_{k,i}, \mathbf{y}_{k,i}, \boldsymbol{\Omega}_{k-1,i})$ will eventually need some sort of additional information to relate the j-th neighboring node measurement to the i-th node states as in the following function:

$$\mathbf{y}_{k,j} = \mathbf{h}_k^{i,j}(\mathbf{x}_{k,i}) \tag{4}$$

If such function can be constructed, then the j-th node measurement can be fused at the i-th node as if it was actually produced by a sensor that is local to the i-th node. This methodology was used in [24] in which the exchanging of position measurements from robots was proposed. The authors verified that it could only be possible if the relative position vectors had to be available. Additionally, in case function $\mathbf{h}_k^{i,j}(\cdot)$ is nonlinear, then it should be linearized about $\hat{\mathbf{x}}_{k|k-1,i}$ as in the extended Kalman filter algorithm.

V. Delayed Measurements

In a distributed sensor network, it is expected that the exchanged measurements will spread across the network and reach distinct nodes with varying time delays. Here, the sample step is small enough such that the node dynamics has been assumed constant between two consecutive sample steps. Thus a delay smaller than the sampling step is negligible [25]. Additionally, if a measurement is received at instant t_l in which $t_{k-n} \leq t_l \leq t_{k-n+1}$, then it has been considered as delayed by n sample steps. Under these assumptions, a measurement with a delay lower than one sample step can be fused as usual. However if a measurement happens to reach a node with a delay higher than the sampling interval, then the local estimate could be severally degraded had the measurement been naïvely fused.

It should be noticed that all previous methodologies need to store information to accomplish the delayed measurement fusion [14], [20], [23]. Thus one must define a maximum allowed delay, thereafter called max. If any measurement with a delay higher than max is received, then it will be discarded.

A. Measurement Grouping

Let $\boldsymbol{\nu}_k^i$ be the set of all measurements that the i-th node received in the instant k. It has been considered that these measurements from the neighboring nodes as described in eq. 4 depend on a function $\mathbf{h}_k^{i,j}(\mathbf{x}_{k,i})$ that is either linear or has been linearized about $\hat{\mathbf{x}}_{k|k-1,i}$, thus $\mathbf{y}_{k,j} = \mathbf{H}_k^{i,j}\mathbf{x}_{k,i} + \mathbf{v}_{k,j}$. The aforementioned set can be partitioned into subsets according to the measurement delay, hereafter called $\boldsymbol{\nu}_{k,\Delta_n}^i$. Thus the subset $\boldsymbol{\nu}_{k,\Delta_n}^i$ is composed of all measurements received by the i-th node in the instant k delayed by Δ_n sample steps, where $0 \leq \Delta_0 < \Delta_1 < \cdots < \Delta_L \leq max$.

The measurements in the same subset $\boldsymbol{\nu}_{k,\Delta_n}^i$ can be additionally fused into one single vector to reduce the computational burden as in eqs. 5:

$$
\begin{aligned}
\mathbf{y}_{k,\Delta_n,i}^f &= \sum_{j\in\boldsymbol{\nu}_{k,\Delta_n}^i} \mathbf{H}_{k-\Delta_n}^{i,j,T}\mathbf{R}_{k-\Delta_n,j}^{-1}\mathbf{y}_{k-\Delta_n,j} = \\
&= \left(\sum_{j\in\boldsymbol{\nu}_{k,\Delta_n}^i} \mathbf{H}_{k-\Delta_n}^{i,j,T}\mathbf{R}_{k-\Delta_n,j}^{-1}\mathbf{H}_{k-\Delta_n}^{i,j}\right)\mathbf{x}_{k-\Delta_n,i} + \\
&+ \sum_{j\in\boldsymbol{\nu}_{k,\Delta_n}^i} \mathbf{H}_{k-\Delta_n}^{i,j,T}\mathbf{R}_{k-\Delta_n,j}^{-1}\mathbf{v}_{k-\Delta_n,j} = \\
&= \mathbf{H}_{k,\Delta_n,i}^f\mathbf{x}_{k-\Delta_n,i} + \mathbf{v}_{k,\Delta_n,i}^f
\end{aligned} \tag{5a}
$$

$$
\begin{aligned}
\mathbf{R}_{k,\Delta_n,i}^f &= cov\{\mathbf{y}_{k,\Delta_n,i}^f\mathbf{y}_{k,\Delta_n,i}^{f,T}\} = \\
&= \left(\sum_{j\in\boldsymbol{\nu}_{k,\Delta_n}^i} \mathbf{H}_{k-\Delta_n}^{i,j,T}\mathbf{R}_{k-\Delta_n,j}^{-1}\mathbf{H}_{k-\Delta_n}^{i,j}\right) = \mathbf{H}_{k,\Delta_n,i}^f
\end{aligned} \tag{5b}
$$

in which the information form of the Kalman filter should be used, or as in eq. 6 if all measurements in the set share the same measurement matrix [26]:

$$
\begin{cases}
\mathbf{R}_{k,\Delta_n,i}^{f,-1} = \displaystyle\sum_{j\in\boldsymbol{\nu}_{k,\Delta_n}^i} \mathbf{R}_{k-\Delta_n,j}^{-1} \\
\mathbf{y}_{k,\Delta_n,i}^f = \mathbf{R}_{k,\Delta_n,i}^f\left[\displaystyle\sum_{j\in\boldsymbol{\nu}_{k,\Delta_n}^i} \mathbf{R}_{k-\Delta_n,j}^{-1}\mathbf{y}_{k-\Delta_n,j}\right]
\end{cases} \tag{6}
$$

Finally, the problem is reduced to fuse the measurements $\mathbf{y}_{k,\Delta_n,i}^f$, $n \in [0,1,2,\cdots,L]$ and to compute (or to approximate) the p.d.f. $p(\mathbf{x}_{k,i}|\mathbf{y}_{k,\Delta_0,i}^f, \mathbf{y}_{k,\Delta_1,i}^f, \cdots, \mathbf{y}_{k,\Delta_L,i}^f, \boldsymbol{\Omega}_{k-1,i}) = p(\mathbf{x}_{k,i}|\boldsymbol{\Omega}_{k,i})$.

One should note that a consensus over the network is not pursued here as in [1] or [2]. The nodes send to the neighbors the local measurements by the time they are acquired. Additionally, a node can retransmit the information received to permit that a measurement reach, even if delayed, nodes outside its neighborhood. The idea is to fuse all available information (delayed or not) without waiting for the communication steps to achieve the network consensus.

B. The Reiterated Kalman Filter

When node of a distributed sensor network receives a delayed measurement, then the optimal fusion is accomplished if the posterior estimate is exactly the same as it would be if the measurement had been received at the time of its production, without the delay. The most direct way to accomplish that is to reiterate the Kalman filter from the instant when the measurement was produced until the present time [23]. However, one should notice that the MMSE optimality is assured only in linear and Gaussian systems.

The aforementioned methodology can be only used if the updated estimates and covariance matrices together with the fused measurements and respective statistics are stored from instant $k-max$ up to instant $k-1$. Let $\mathbf{y}_{k-n,i}^u$ and $\mathbf{R}_{k-n,i}^u$ be, respectively, the measurement vector and its covariance that was used in the Kalman filter update step at instant $k-n$ by the i-th node. Thus the algorithm can be written as follows:

- $j = \Delta_L$, $n = L$
- WHILE $j \geq 0$
  - IF $j = \Delta_n$ THEN
    - $n = n - 1$
    - Fuse the measurement vectors $\mathbf{y}_{k-j,i}^u$ and $\mathbf{y}_{k,j,i}^f$ into $\mathbf{y}_{k,j,i}^d$.
    - Fuse the statistics of the measurement vectors $\mathbf{R}_{k-j,i}^u$ and $\mathbf{R}_{k,j,i}^f$ into $\mathbf{R}_{k,j,i}^d$.
  - ELSE
    - $\mathbf{y}_{k,j,i}^d = \mathbf{y}_{k-j,i}^u$

- * $\mathbf{R}^d_{k,j,i} = \mathbf{R}^u_{k-j,i}$
- ENDIF
- Using $\mathbf{y}^d_{k,j,i}$, $\mathbf{R}^d_{k,j,i}$, $\hat{\mathbf{x}}_{k-j|k-j-1,i}$, and $\mathbf{P}_{k-j|k-j-1,i}$ apply the update step of the Kalman filter and overwrite $\hat{\mathbf{x}}_{k-j|k-j,i}$ and $\mathbf{P}_{k-j|k-j,i}$.
- Apply the propagation step of the Kalman filter and overwrite $\hat{\mathbf{x}}_{k-j+1|k-j,i}$ and $\mathbf{P}_{k-j+1|k-j,i}$.
- $\mathbf{y}^u_{k-j,i} = \mathbf{y}^d_{k,j,i}$
- $\mathbf{R}^u_{k-j,i} = \mathbf{R}^d_{k,j,i}$
- j = j - 1

- ENDWHILE

If the node does not receive any measurements delayed more than max sampling steps, then the posterior estimate will be optimal in the MMSE sense in a linear and Gaussian system. However the computational workload is huge. If the most delayed measurement was produced n sampling steps in the past, then this algorithm will iterate the Kalman filter $n+1$ times.

C. Measurement Transportation [27]

A novel approach to the fusion of delayed measurements in the Kalman filter is proposed here: the measurement transportation. The algorithm, though suboptimal in the MMSE sense, has achieved a good performance in the situations of interest with lighter computational load and less storage necessity than the reiterated Kalman filter. The approach is based on the technique in [22] and on the delayed-state Kalman filter [21], which was constructed to fuse a measurement composed of two consecutive states, $\mathbf{x}_{k-1}$ and $\mathbf{x}_k$.

Using the model in eq. 1, the state $\mathbf{x}_{k-n,i}$ can be related to $\mathbf{x}_{k,i}$ as in eq. 7:

$$\begin{aligned}\mathbf{x}_{k-n,i} = &\left[\prod_{l=0}^{n-1} \mathbf{F}^{-1}_{k-(n-l),i}\right]\mathbf{x}_{k,i} - \\ &\sum_{j=1}^{n}\left(\left[\prod_{l=0}^{n-j} \mathbf{F}^{-1}_{k-(n-l),i}\right]\mathbf{G}_{k-j,i}\mathbf{w}_{k-j,i}\right) - \\ &\sum_{j=1}^{n}\left(\left[\prod_{l=0}^{n-j} \mathbf{F}^{-1}_{k-(n-l),i}\right]\mathbf{B}_{k-j,i}\mathbf{u}_{k-j,i}\right)\end{aligned} \tag{7}$$

Thus the fused delayed measurement in each subset $\boldsymbol{\nu}^i_{k,\Delta_n}$ can be transported to the present instant by:

$$\mathbf{y}^f_{k,\Delta_n,i} = \mathbf{H}^p_{k,\Delta_n,i}\mathbf{x}_k + \mathbf{u}^p_{k,\Delta_n,i} + \mathbf{v}^p_{k,\Delta_n,i} = \mathbf{y}^p_{k,\Delta_n,i} \tag{8}$$

where:

$$\mathbf{H}^p_{k,\Delta_n,i} = \mathbf{H}^f_{k,\Delta_n,i}\left[\prod_{l=0}^{\Delta_n-1} \mathbf{F}^{-1}_{k-(\Delta_n-l),i}\right]$$

$$\mathbf{u}^p_{k,\Delta_n,i} = -\mathbf{H}^f_{k,\Delta_n,i}\sum_{j=1}^{\Delta_n}\left(\left[\prod_{l=0}^{\Delta_n-j} \mathbf{F}^{-1}_{k-(\Delta_n-l),i}\right]\mathbf{B}_{k-j,i}\mathbf{u}_{k-j,i}\right)$$

$$\mathbf{v}^p_{k,\Delta_n,i} = \mathbf{v}^f_{k,\Delta_n,i} - \underbrace{\mathbf{H}^f_{k,\Delta_n,i}\sum_{j=1}^{\Delta_n}\left(\left[\prod_{l=0}^{\Delta_n-j} \mathbf{F}^{-1}_{k-(\Delta_n-l),i}\right]\mathbf{G}_{k-j,i}\mathbf{w}_{k-j,i}\right)}_{\star}$$

Notice that the fused delayed measurement noise $\mathbf{v}^p_{k,\Delta_n,i}$ has a covariance ellipsoid larger than that of the original measurement due to the summation of the model noise samples from instants $k-\Delta_n$ up to $k-1$ ($\star$). Thus, the fused delayed measurement signal-to-noise ratio degrades with respect to the instantaneous measurement.

By stacking the measurements in each subset $\boldsymbol{\nu}^i_{k,\Delta_n}$, $n \in [0,1,2,\cdots,L]$, the measurement vector to be fused at instant k by the i-th node is:

$$\mathbf{y}^{e,p}_{k,i} = \mathbf{H}^{e,p}_{k,i}\mathbf{x}_{k,i} + \mathbf{v}^{e,p}_{k,i} \tag{9}$$

where:

$$\begin{aligned}\mathbf{y}^{e,p}_{k,i} &= \begin{bmatrix} \mathbf{y}^{p,T}_{k,\Delta_0,i} & \mathbf{y}^{p,T}_{k,\Delta_1,i} & \cdots & \mathbf{y}^{p,T}_{k,\Delta_L,i}\end{bmatrix}^T - \mathbf{u}^{e,p}_{k,i} \\ \mathbf{u}^{e,p}_{k,i} &= \begin{bmatrix} \mathbf{u}^{p,T}_{k,\Delta_0,i} & \mathbf{u}^{p,T}_{k,\Delta_1,i} & \cdots & \mathbf{u}^{p,T}_{k,\Delta_L,i}\end{bmatrix}^T \\ \mathbf{H}^{e,p}_{k,i} &= \begin{bmatrix} \mathbf{H}^{p,T}_{k,\Delta_0,i} & \mathbf{H}^{p,T}_{k,\Delta_1,i} & \cdots & \mathbf{H}^{p,T}_{k,\Delta_L,i}\end{bmatrix}^T \\ \mathbf{v}^{e,p}_{k,i} &= \begin{bmatrix} \mathbf{v}^{p,T}_{k,\Delta_0,i} & \mathbf{v}^{p,T}_{k,\Delta_1,i} & \cdots & \mathbf{v}^{p,T}_{k,\Delta_L,i}\end{bmatrix}^T\end{aligned}$$

Under the foregoing assumptions, it is clear that $\mathbf{v}^{e,p}_{k,i}$ has zero mean. Thus its covariance matrix is:

$$\begin{aligned}\mathbf{R}^{e,p}_{k,i} &= E\{\mathbf{v}^{e,p}_{k,i}\mathbf{v}^{e,p,T}_{k,i}\} = \\ &= \begin{bmatrix} E\{\mathbf{v}^p_{k,\Delta_0,i}\mathbf{v}^{p,T}_{k,\Delta_0,i}\} & \cdots & E\{\mathbf{v}^p_{k,\Delta_0,i}\mathbf{v}^{p,T}_{k,\Delta_L,i}\} \\ \vdots & \ddots & \vdots \\ E\{\mathbf{v}^p_{k,\Delta_L,i}\mathbf{v}^{p,T}_{k,\Delta_0,i}\} & \cdots & E\{\mathbf{v}^p_{k,\Delta_L,i}\mathbf{v}^{p,T}_{k,\Delta_L,i}\}\end{bmatrix}\end{aligned} \tag{10}$$

where the expectations $E\{\mathbf{v}^p_{k,\Delta_n,i}\mathbf{v}^{p,T}_{k,\Delta_m,i}\}$, $n,m \in [0,1,2,\cdots,L]$, can be computed as follows:

$$E\{\mathbf{v}^p_{k,n,i}\mathbf{v}^{p,T}_{k,m,i}\} = \begin{cases} \mathbf{R}^f_{k,n,i}\cdot\delta(n-m) + \mathbf{H}^f_{k,n,i}\cdot \\ \quad \cdot \displaystyle\sum_{j=1}^{min(n,m)}\left(\left[\prod_{i=0}^{n-j}\mathbf{F}^{-1}_{k-(n-i)}\right]\mathbf{Q}_{k-j}\cdot\right. \\ \quad \left.\cdot\left[\prod_{i=0}^{m-j}\mathbf{F}^{-1}_{k-(m-i)}\right]^T\right)\mathbf{H}^{T,f}_{k,m,i}, \quad n>0, m>0 \\ \mathbf{R}^f_{k,0,i}\cdot\delta(n)\cdot\delta(m), \quad m=0 \text{ or } n=0\end{cases} \tag{11}$$

where $\delta(n)$ is the Kronecker's delta.

The usual Kalman filter algorithm cannot be used with the measurement in eq. 9, because the measurement noise $\mathbf{v}^{e,p}_{k,i}$ is not uncorrelated with the model noise. Thus, the linear MMSE estimate produced by the Kalman filter update step, defined in eq. 12, needs to be rewritten [28].

$$\begin{cases} \hat{\mathbf{x}}_{k|k,i} = E\{\mathbf{x}_{k,i}|\mathbf{y}^{e,p}_{k,i}, \mathbf{\Omega}_{k-1,i}\} = E\{\mathbf{x}_{k,i}|\mathbf{\Omega}_{k-1,i}\}+ \\ \quad + \mathbf{C}^{xy}_{k,i}\mathbf{C}^{yy,-1}_{k,i}(\mathbf{y}^{e,p}_{k,i} - E\{\mathbf{y}^{e,p}_{k,i}|\mathbf{\Omega}_{k-1,i}\}) \\ \mathbf{C}^{xy}_{k,i} = E\{(\mathbf{x}_{k,i} - E\{\mathbf{x}_{k,i}|\mathbf{\Omega}_{k-1,i}\})\cdot \\ \quad \cdot (\mathbf{y}^{e,p}_{k,i} - E\{\mathbf{y}^{e,p}_{k,i}|\mathbf{\Omega}_{k-1,i}\})^T|\mathbf{\Omega}_{k-1,i}\} \\ \mathbf{C}^{yy}_{k,i} = E\{(\mathbf{y}^{u}_{k,i} - E\{\mathbf{y}^{e,p}_{k,i}|\mathbf{\Omega}_{k-1,i}\})\cdot \\ \quad \cdot (\mathbf{y}^{e,p}_{k,i} - E\{\mathbf{y}^{e,p}_{k,i}|\mathbf{\Omega}_{k-1,i}\})^T|\mathbf{\Omega}_{k-1,i}\} \\ \mathbf{P}_{k|k,i} = \mathbf{P}_{k|k-1,i} - \mathbf{C}^{xy}_{k,i}\mathbf{C}^{yy,-1}_{k,i}\mathbf{C}^{xy,T}_{k,i} \end{cases} \tag{12}$$

One can see that [28], [29]:

$$E\{\mathbf{y}^{e,p}_{k,i}|\mathbf{\Omega}_{k-1,i}\} = \mathbf{H}^{e,p}_{k,i}E\{\mathbf{x}_{k,i}|\mathbf{\Omega}_{k-1,i}\} = \mathbf{H}^{e,p}_{k,i}\hat{\mathbf{x}}_{k|k-1,i} \tag{13}$$

$$\mathbf{C}^{xy}_{k,i} = \mathbf{P}_{k|k-1,i}\mathbf{H}^{e,p,T}_{k,i} + \mathbf{S}_{k,i} \tag{14}$$

$$\mathbf{C}^{yy}_{k,i} = \mathbf{H}^{e,p}_{k,i}\mathbf{P}_{k|k-1,i}\mathbf{H}^{e,p,T}_{k,i} + \mathbf{R}^{e,p}_{k,i} + \mathbf{H}^{e,p}_{k,i}\mathbf{S}_{k,i} + \mathbf{S}^{T}_{k,i}\mathbf{H}^{e,p,T}_{k,i} \tag{15}$$

where $\mathbf{S}_{k,i} = E\{(\mathbf{x}_{k,i} - \hat{\mathbf{x}}_{k|k-1,i})\mathbf{v}^{e,p,T}_{k,i}|\mathbf{\Omega}^{i}_{k-1}\}$. In the usual Kalman filter algorithm, $\mathbf{S}_{k,i}$ is zero due to the assumption that the model and measurement noise vectors are uncorrelated. However, the transported measurement, defined in eq. 9, carries the model noises from the instant it was produced up to the instant $k-1$.

The $\mathbf{S}_{k,i}$ matrix can be rewritten as:

$$\begin{aligned} \mathbf{S}_{k,i} = E\{(\mathbf{x}_{k,i} - E\{\mathbf{x}_{k,i}\})\mathbf{v}^{e,p,T}_{k,i}|\mathbf{\Omega}_{k-1,i}\}- \\ E\{(\hat{\mathbf{x}}_{k|k-1,i} - E\{\mathbf{x}_{k,i}\})\mathbf{v}^{e,p,T}_{k,i}|\mathbf{\Omega}_{k-1,i}\} \end{aligned} \tag{16}$$

It can be verified that $\hat{\mathbf{x}}_{k|k-1,i}$ is a random vector that depends just on all the measurement vectors fused up to instant $k-1$ at the i-th node and on the random vector $\mathbf{x}_{0,i}$. The latter has been assumed to be independent with respect to all measurements and model noise sequences throughout the network. Thus, conditioned on $\mathbf{\Omega}_{k-1,i}$, $\hat{\mathbf{x}}_{k|k-1,i}$ and $\mathbf{v}^{e,p}_{k,i}$ are independent, which leads to $E\{(\hat{\mathbf{x}}_{k|k-1,i} - E\{\mathbf{x}_k\})\mathbf{v}^{e,p,T}_{k,i}|\mathbf{\Omega}_{k-1,i}\} = \mathbf{0}_{M_i\times(L+1)N_i}$.

Additionally it can be shown by induction that:

$$\begin{aligned} \mathbf{x}_{k,i} = &\left[\prod_{t=1}^{n}\mathbf{F}_{k-t,i}\right]\mathbf{x}_{k-n,i}+ \\ &\mathbf{G}_{k-1,i}\mathbf{w}_{k-1,i} + \mathbf{B}_{k-1,i}\mathbf{u}_{k-1,i}+ \\ &\sum_{j=2}^{n}\left(\left[\prod_{t=1}^{j-1}\mathbf{F}_{k-t,i}\right]\mathbf{G}_{k-j,i}\mathbf{w}_{k-j,i}\right)+ \\ &\sum_{j=2}^{n}\left(\left[\prod_{t=1}^{j-1}\mathbf{F}_{k-t,i}\right]\mathbf{B}_{k-j,i}\mathbf{u}_{k-j,i}\right) \end{aligned} \tag{17}$$

and setting $n = k$, one can see that:

$$\begin{aligned} \mathbf{x}_{k,i} - E\{\mathbf{x}_{k,i}\} = \left[\prod_{t=1}^{k}\mathbf{F}_{k-t,i}\right](\mathbf{x}_{0,i} - \mathbf{m}_{0,i})+ \\ \mathbf{G}_{k-1,i}\mathbf{w}_{k-1,i} + \sum_{j=2}^{k}\left(\left[\prod_{t=1}^{j-1}\mathbf{F}_{k-t,i}\right]\mathbf{G}_{k-j,i}\mathbf{w}_{k-j,i}\right) \end{aligned} \tag{18}$$

A white sequence has been assumed as the model noise $\mathbf{G}_k\mathbf{w}_k$, $k \in \mathbb{N}$. Thus $E\{\mathbf{G}_n\mathbf{w}_n\mathbf{w}^T_m\mathbf{G}^T_m\} = \mathbf{Q}_n \cdot \delta(n-m)$. This result together with the assumption that $\mathbf{x}_0$ is independent with respect to all model and measurement noise sequences leads to:

$$\begin{aligned} &E\{(\mathbf{x}_{k,i} - E\{\mathbf{x}_{k,i}\})\mathbf{v}^{p,T}_{k,\Delta_n,i}|\mathbf{\Omega}_{k-1,i}\} = \\ &\left\{-\mathbf{Q}_{k-1}\left[\prod_{l=0}^{\Delta_n-1}\mathbf{F}^{-1}_{k-(\Delta_n-l),i}\right]^T - \sum_{j=2}^{\Delta_n}\left(\left[\prod_{t=1}^{j-1}\mathbf{F}_{k-t,i}\right]\cdot\right.\right. \\ &\left.\left.\cdot\mathbf{Q}_{k-j}\left[\prod_{l=0}^{\Delta_n-j}\mathbf{F}^{-1}_{k-(\Delta_n-l),i}\right]^T\right)\right\}\mathbf{H}^{f,T}_{k,\Delta_n,i} \end{aligned} \tag{19}$$

for $n \in [0, 1, 2, \cdots, L]$ and $\Delta_n \neq 0$. If $\Delta_0 = 0$, then:

$$E\{(\mathbf{x}_{k,i} - E\{\mathbf{x}_{k,i}\})\mathbf{v}^{p,T}_{k,\Delta_0,i}|\mathbf{\Omega}_{k-1,i}\} = \mathbf{0}_{M_i\times N_i} \tag{20}$$

The results in eqs. 19 and 20 allow the computation of the matrix $\mathbf{S}_{k,i}$ as in eq. 21:

$$\mathbf{S}_{k,i} = \begin{bmatrix} \left(E\{(\mathbf{x}_{k,i} - E\{\mathbf{x}_{k,i}\})\mathbf{v}^{p,T}_{k,\Delta_0,i}|\mathbf{\Omega}_{k-1,i}\}\right)^T \\ \left(E\{(\mathbf{x}_{k,i} - E\{\mathbf{x}_{k,i}\})\mathbf{v}^{p,T}_{k,\Delta_1,i}|\mathbf{\Omega}_{k-1,i}\}\right)^T \\ \vdots \\ \left(E\{(\mathbf{x}_{k,i} - E\{\mathbf{x}_{k,i}\})\mathbf{v}^{p,T}_{k,\Delta_L,i}|\mathbf{\Omega}_{k-1,i}\}\right)^T \end{bmatrix}^T \tag{21}$$

Finally the Kalman filter update step can be performed using the linear MMSE estimate in eq. 12, which can be computed using eqs. 13, 14, and 15.

This method needs the product of the inverse of consecutive state-transition matrices, which imposes a heavy computational load. However, the state-transition matrix inverses from instant $k - max$ up to instant $k-1$ can be stored to decrease the computational burden of computing these products. One should notice that the state-transition matrix is always invertible for discretized continuous linear systems [30].

Table II in [20] shows the memory needs for nine algorithms that can fuse delayed measurements in a multisensor environment. Local node access to the state-transition matrix and model noise covariance matrices from instant $k - max$ up to instant $k-1$ has been assumed. Thus, if it holds, then the measurement transportation just need to store $max \cdot M_i$ elements regarding the control signals. If the state-transition matrix inverses are also stored to decrease the computational burden, then the proposed algorithm must store $max \cdot (M_i + M_i^2)$ elements. In both cases, the measurement transportation is the method with the lowest memory needs among the methods analyzed in [20].

The MMSE estimate could be achieved in a linear and Gaussian system if all the measurements fused with Kalman filtering were not delayed, which is not the case of the investigated scenarios. No claim of optimality is made regarding the use of either the reiterated Kalman filtering or the measurement transportation approach in the investigated scenarios where error dynamics are linearized, noise sequences are non-Gaussian, and delayed measurements transit throughout the network. However, since the equations have been derived based on linear MMSE estimation, it can be claimed that the measurement transportation approach is an unbiased estimator for the fusion of delayed measurements [28].

VI. UAV FLEET PROBLEM FORMULATION

If a fleet of UAVs is modeled as nodes of a distributed sensor network with links to exchange information, then it has been indicated by eq. 4 and its further development that GPS measurements from one UAV can be used by another UAV if their relative positions are available measurements as well. This information sharing can be used to increase the robustness of the fleet formation flight, e.g. if a UAV loses GPS signal lock, then INS solution errors can be limited if the neighboring nodes' GPS measurements are correctly fused. However, it is likely that these network data will arrive with varying, possibly high delays across the network nodes. Thus, the scenario motivates the use of the algorithms in the last section to properly fuse the delayed information in transit throughout the network.

Omitting model noise, the continuous-time INS error model dynamics for the *i*-th UAV is described as follows [31], [32]:

$$\begin{aligned} \dot{\mathbf{x}}_i(t) &= \mathbf{A}_i(t)\cdot\mathbf{x}_i(t) \\ \mathbf{A}_i &= \left[\begin{array}{c|c|c|c|c} [\boldsymbol{\rho}_{l,i}]_\times & \mathbf{I}_{3\times3} & \mathbf{0}_{3\times3} & \mathbf{0}_{3\times3} & \mathbf{0}_{3\times3} \\ \mathbf{g}_{e,i} & \boldsymbol{\alpha}_i & \boldsymbol{\Gamma}_i & \mathbf{D}^b_{l,i} & \mathbf{0}_{3\times3} \\ \mathbf{0}_{3\times3} & \mathbf{0}_{3\times3} & \boldsymbol{\beta}_i & \mathbf{0}_{3\times3} & -\mathbf{D}^b_{l,i} \\ \mathbf{0}_{3\times3} & \mathbf{0}_{3\times3} & \mathbf{0}_{3\times3} & \mathbf{0}_{3\times3} & \mathbf{0}_{3\times3} \\ \mathbf{0}_{3\times3} & \mathbf{0}_{3\times3} & \mathbf{0}_{3\times3} & \mathbf{0}_{3\times3} & \mathbf{0}_{3\times3} \end{array}\right] \\ \mathbf{x}_i &= \left[\begin{array}{ccccc} \Delta\mathbf{R}^T_{l,i} & \Delta\mathbf{V}^T_{l,i} & \boldsymbol{\psi}^T_i & \boldsymbol{\nabla}^T_{b,i} & \boldsymbol{\epsilon}^T_{b,i} \end{array}\right]^T \end{aligned} \tag{22}$$

where $\boldsymbol{\alpha}_i = [\boldsymbol{\rho}_{l,i} + 2\boldsymbol{\Omega}_{e,l,i}]_\times$, $\boldsymbol{\beta}_i = [\boldsymbol{\rho}_{l,i} + \boldsymbol{\Omega}_{e,l,i}]_\times$, $\boldsymbol{\sigma}_i = [\mathbf{Asp}_{l,i}]_\times$, $\mathbf{g}_{e,i} = diag(-g_{e,i}/R_{e,i} \;\; -g_{e,i}/R_{e,i} \;\; 2g_{e,i}/R_{e,i})$, and $diag(\cdot)$ is a diagonal matrix. Thus the discrete form of this model can be written as:

$$\mathbf{x}_{k+1,i} = \mathbf{F}_{k,i}\mathbf{x}_{k,i} + \mathbf{u}_{k,i} + \mathbf{G}_{k,i}\mathbf{w}_{k,i} \tag{23}$$

where $\mathbf{x}_{k,i} = \mathbf{x}_i(t_k)$, $\mathbf{F}_{k,i} = e^{\mathbf{A}(t_{k-1})\cdot\Delta}$, Δ is the sample step, $\mathbf{G}_{k,i}\mathbf{w}_{k,i}$ is the model noise as described in eq. 1, and $\mathbf{u}_{k,i}$ is a virtual control vector used to remove the mean of $\mathbf{x}_{k,i}$ when the Kalman filter estimates are fed back to correct the INS.

The GPS measurement is assumed to directly provide UAV position and velocity in the WGS-84 ellipsoid Earth-fixed coordinate frame. Thus, these data are compared to the INS solution to produce a measurement vector of the state-error. Receiver clock errors have not been involved in this investigation. Under this considerations, the discrete GPS measurement equation for the INS error model is:

$$\begin{aligned} \mathbf{y}^{GPS}_{k,i} &= \left[\begin{array}{c} \mathbf{D}^e_{l,i}(\mathbf{p}^{GPS}_{k,e,i} - \mathbf{p}^{INS}_{k,e,i}) \\ \mathbf{D}^e_{l,i}(\mathbf{v}^{GPS}_{k,e,i} - \mathbf{v}^{INS}_{k,e,i}) \end{array}\right] \\ \mathbf{y}^{GPS}_{k,i} &= \left[\begin{array}{ccccc} \mathbf{I}_3 & \mathbf{0}_3 & \mathbf{0}_3 & \mathbf{0}_3 & \mathbf{0}_3 \\ \mathbf{0}_3 & \mathbf{I}_3 & \mathbf{0}_3 & \mathbf{0}_3 & \mathbf{0}_3 \end{array}\right]\mathbf{x}_{k,i} + \\ &+ \left[\begin{array}{cc} \mathbf{D}^e_{l,i} & \mathbf{0}_3 \\ \mathbf{0}_3 & \mathbf{D}^e_{l,i} \end{array}\right]\mathbf{v}^{GPS}_{k,i} \end{aligned} \tag{24}$$

where $\mathbf{p}^{GPS}_{k,e,i}$ and $\mathbf{v}^{GPS}_{k,e,i}$ are, respectively, the position and velocity of the vehicle given by the GPS receiver on board and represented in the Earth-Centered-Earth-Fixed coordinate frame; $\mathbf{p}^{INS}_{k,e,i}$ and $\mathbf{v}^{INS}_{k,e,i}$ are, respectively, the position and velocity of the vehicle given by the INS and represented in the Earth-Centered-Earth-Fixed coordinate frame; and $\mathbf{v}^{GPS}_{k,i}$ is assumed to be a white Gaussian noise sequence with covariance $\mathbf{R}^{GPS}_{k,i}$. The DCM $\mathbf{D}^e_{l,i}$ can be computed using either the GPS data or the INS solution.

If the *i*-th UAV receives the GPS position from the *j*-th UAV ($\mathbf{p}^{GPS}_{k,e,j}$), then the former can use this information if the measurement of the relative position between the two UAVs ($\mathbf{p}_{k,e,j\to i}$) is available as in eq. 25:

$$\mathbf{p}^{GPS}_{k,e,j} + \mathbf{p}_{k,e,j\to i} = \mathbf{p}^{GPS,i}_{k,e,j} \tag{25}$$

where $\mathbf{p}^{GPS,i}_{k,e,j}$ is a position measurement of the *i*-th UAV using the GPS measurement data from *j*-th UAV and the measurement of the relative position between the UAVs. The latter cannot be constructed using the GPS information from both UAVs, since then no additional information would be available. The relative position can be obtained, for example, from an imaging pod and proper image processing, or by a RF range measurement as studied in [33]. Finally, the state-error measurement using the information from the *j*-th UAV can be constructed as follows:

$$\begin{aligned} \mathbf{y}^{GPS,i}_{k,j} &= \mathbf{D}^e_{l,i}(\mathbf{p}^{GPS,i}_{k,e,j} - \mathbf{p}^{INS}_{k,e,i}) \\ \mathbf{y}^{GPS,i}_{k,j} &= \left[\begin{array}{ccccc} \mathbf{I}_3 & \mathbf{0}_3 & \mathbf{0}_3 & \mathbf{0}_3 & \mathbf{0}_3 \end{array}\right]\mathbf{x}_{k,i} + \mathbf{D}^e_{l,i}\mathbf{v}^{GPS,i}_{k,j} \end{aligned} \tag{26}$$

where $\mathbf{v}^{GPS,i}_{k,j}$ is assumed to be a white Gaussian noise sequence with $\mathbf{R}^{GPS,i}_{k,j}$ covariance matrix

If the measurement from the *j*-th UAV arrives with delay, then the algorithms showed previously can be used to correctly fuse it into the *i*-th UAV Kalman filter. One should notice that the relative positions and the GPS data does not need to be transmitted at the same time. However, the UAVs must store the relative positions received from instant $k - max$ up to instant k to properly convert the neighboring nodes' GPS measurements as described in eq. 25 when needed.

VII. SIMULATIONS AND RESULTS

The simulations have been carried out using a swarm of 5 UAVs. The INS solution was given by the algorithm in [34]. Additionally, a magnetometer as described in [35] has been added to each UAV to limit the misalignment due to the low-quality inertial sensors. The communication links are shown in fig. 1, the simulations parameters are presented in Table I, and the UAVs velocities and angular rates are described in the Apendix.

The UAVs do not share any information before $t = 151$ s. Additionally, all the measurements have been considered to propagate within the network and reach neighboring nodes at a fixed 60 s (6,000 sampling steps) after measurement transmission, which is the maximum allowed delay. This is assumed to be the worst scenario possible, and provides

TABLE I

SIMULATION PARAMETERS

Sensors	
$\boldsymbol{\nabla}$	$\begin{bmatrix} 3 & 3 & 3 \end{bmatrix}^T$ mg
$\boldsymbol{\epsilon}$	$\begin{bmatrix} 1000 & 1000 & 1000 \end{bmatrix}^T$ $\circ$/h
Accelerometers covariance ($\mathbf{R}_{\boldsymbol{\nabla}}$)	$diag\begin{pmatrix} 1 & 1 & 1 \end{pmatrix}$ $(mg)^2$
Rate-gyros covariance ($\mathbf{R}_{\boldsymbol{\epsilon}}$)	$diag\begin{pmatrix} 500 & 500 & 500 \end{pmatrix}$ $(\circ/\mathrm{h})^2$
$\mathbf{R}_{GPS}$	$diag\begin{pmatrix} 81 & 81 & 81 & 0.1 & 0.1 & 0.1 \end{pmatrix}$ SI units^2
$\mathbf{R}_{magnetometer}$	$diag\begin{pmatrix} (2\cdot10^{-5})^2 & (2\cdot10^{-5})^2 & (2\cdot10^{-5})^2 \end{pmatrix}$ Gauss^2
Covariance of relative position measurement	$5\cdot diag\begin{pmatrix} 81 & 81 & 81 \end{pmatrix}$ m^2
GPS and magnetometer data frequency	1 Hz
INS	
Initial position	$23°12'\ S\ \ 45°52'\ W + 0.05\cdot\mathcal{G}$ where $\mathcal{G}$ is a zero-mean Gaussian variable with standard deviation of 1".
Initial altitude	700 m $+\ \mathcal{H}$ where $\mathcal{H}$ is a zero-mean Gaussian variable with standard deviation of 1 m.
Initial velocity	$\begin{bmatrix} 0 & 0 & 0 \end{bmatrix}^T$ m/s
Initial alignment	TRIAD algorithm [36]
INS solution sampling rate (t_{ins})	0.01 s
Kalman filter	
Feedback start	95 s
$\mathbf{Q}$, $t < 95$ s	$1/50\cdot t_{ins}\cdot\left[\begin{array}{cc} \mathbf{0}_3 & \mathbf{0}_3 \\ \mathbf{D}_l^b & \mathbf{0}_3 \\ \mathbf{0}_3 & -\mathbf{D}_l^b \\ \hline \multicolumn{2}{c}{\mathbf{0}_6} \end{array}\right]\cdot\begin{bmatrix} \mathbf{R}_{\boldsymbol{\nabla}} & \mathbf{0}_3 \\ \mathbf{0}_3 & \mathbf{R}_{\boldsymbol{\epsilon}} \end{bmatrix}\cdot\left[\begin{array}{cc} \mathbf{0}_3 & \mathbf{0}_3 \\ \mathbf{D}_l^b & \mathbf{0}_3 \\ \mathbf{0}_3 & -\mathbf{D}_l^b \\ \hline \multicolumn{2}{c}{\mathbf{0}_6} \end{array}\right]^T$ SI Units^2
$\mathbf{Q}$, $t \geq 95$ s	$1/150\cdot t_{ins}\cdot\left[\begin{array}{cc} \mathbf{0}_3 & \mathbf{0}_3 \\ \mathbf{D}_l^b & \mathbf{0}_3 \\ \mathbf{0}_3 & -\mathbf{D}_l^b \\ \hline \multicolumn{2}{c}{\mathbf{0}_6} \end{array}\right]\cdot\begin{bmatrix} \mathbf{R}_{\boldsymbol{\nabla}} & \mathbf{0}_3 \\ \mathbf{0}_3 & \mathbf{R}_{\boldsymbol{\epsilon}} \end{bmatrix}\cdot\left[\begin{array}{cc} \mathbf{0}_3 & \mathbf{0}_3 \\ \mathbf{D}_l^b & \mathbf{0}_3 \\ \mathbf{0}_3 & -\mathbf{D}_l^b \\ \hline \multicolumn{2}{c}{\mathbf{0}_6} \end{array}\right]^T$ SI Units^2
Initial covariance	$diag\begin{pmatrix} 50^2 & 50^2 & 50^2 & 2^2 & 2^2 & 2^2 & 0.05 & 0.05 & 0.05 & 0.09 & 0.09 & 0.09 & 0.015 & 0.015 & 0.015 \end{pmatrix}$ SI Units^2
Initial estimate	$\mathbf{0}_{15\times1}$ SI units

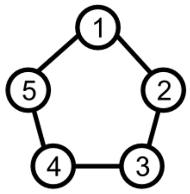

Fig. 1. UAV fleet communication links.

a tough test for the algorithms. Furthermore, UAV 5 loses its GPS lock after $t = 190$ s, and thus the embarked magnetometer data and the delayed measurements vectors from neighboring UAVs 1 and 4 are the only information available to UAV 5. The RMS error of each component of UAV 5's state vector has been used to compare the performance of both the reiterated Kalman filter and the measurement transportation approach.

In the first scenario, all the measurements were fused neglecting the measurement delay. The RMS errors of the position error components computed via a Monte Carlo simulation with 100 realizations are presented in fig. 2. The estimate diverges after the local GPS fault when the delayed measurements are naïvely fused.

In the second scenario, the measurements were fused using the algorithms presented previously. The RMS errors of the state vector components computed via a Monte Carlo simulation with 100 realizations are presented in figs. 3 to 7. The computational load of the reiterated Kalman filter was 3.42 times that of the measurement transportation approach.

A. *Results analysis*

Firstly, fig. 2 clearly shows that the fusion of delayed measurements without adequate processing yields in estimation divergence. On the other hand, the results obtained with scenario 02 and displayed in figs. 3 to 7 show that the algorithms described here correctly fuse the delayed measurements and provide limited navigation errors.

The fusion of neighboring nodes' measurements received by UAV 5 when its GPS observables were available did not provide any noticeable improvement in estimation accuracy ($151s < t < 190s$) because the simulated scenario had the relative position measurement covariance with much larger eigenvalues than those of the GPS measurement covariance. On the other hand, adequate processing of delayed network data from neighboring nodes successfully eliminated estimation divergence when the GPS signal was denied to UAV 5.

Figures 3 to 7 also show that the Kalman filter reiteration, which is optimal in the linear Gaussian case, most times achieved better performance than that of the measurement transportation approach. The cost-benefit ratio of the latter is far more attractive, however, due to its reduced computational workload and statistically similar estimation performance.

VIII. CONCLUSIONS

This paper presented a novel suboptimal approach, called measurement transportation, to fuse delayed measurements in distributed sensor networks. This new technique has less memory needs than the usual algorithms investigated in [20] and a good overall performance is achieved for the problems of interest.

The novel algorithm was compared with the classical approach to fuse delayed measurements in distributed sensor networks: the reiterated Kalman filter. The comparison was carried out using a simulated distributed sensor network that consists of a UAV fleet in formation flight in which the GPS measurements and relative positions are exchanged among neighboring network nodes.

The results shows that both algorithms could correctly fuse the delayed measurements in the proposed scenario and produced similar estimation accuracies. The measurement transportation approach demands a much lower computational load and requires less memory.

One must notice that the distributed estimation problem tackled here is neither Gaussian nor linear. Thus, one should expect that other estimators may yield improved accuracy with respect to that of the reiterated Kalman filter in the scenario simulated here. For example, enhanced accuracy is expected if the INS algorithm is reiterated together with the Kalman filter and the linearization of the error dynamics model about the reiterated INS solution is also carried out at every step. However, the computational load of such estimator algorithm has shown to be prohibitive even to computationally resourceful desktop PCs.

APPENDIX
UAVS TRAJECTORY AND ANGULAR MOVEMENT

The UAV trajectory is composed of several segments with a distinct, constant specific force during each one. They are described in Table II in which $\mathcal{A}_1$ and $\mathcal{A}_2$ are uniformly distributed random variables on the interval $[-3, 3]$ m/s^2 that have been sampled at the beginning of each realization for each UAV.

The IMU attitude evolves as described in eqs. 27 in terms of the Euler angles that rotate the local coordinate frame into alignment with the body coordinate frame (yaw, pitch, and roll rotation sequence).

TABLE II
UAVS TRAJECTORY

		Specific forces		
Start (s)	**End** (s)	**N** (m/s^2)	**E** (m/s^2)	**D** (m/s^2)
0	30	0	0	-g
30	70	$\mathcal{A}_1$	0	-g
70	110	0	$\mathcal{A}_1$	-g
110	150	$\mathcal{A}_1$	$\mathcal{A}_1$	-g
150	190	0	0	-g-$\mathcal{A}_1$
190	240	0	0	-g
240	280	-$\mathcal{A}_1$	0	-g
280	320	0	-$\mathcal{A}_1$	-g
320	360	0	$\mathcal{A}_2$	-g
360	500	0	0	-g+$\mathcal{A}_2$
500	520	0	$\mathcal{A}_2$	-g
520	540	-$\mathcal{A}_2$	0	-g
540	560	-$\mathcal{A}_2$	$\mathcal{A}_2$	-g
560	600	0	-$\mathcal{A}_2$	-g
600	660	0	0	-g-$\mathcal{A}_2$
660	720	0	$\mathcal{A}_2$	-g
720	800	-$\mathcal{A}_2$	0	-g

$$
\begin{aligned}
\psi &= 0.1\sin\left(2\pi\frac{t}{300}\right) + 0.05\sin\left(2\pi\frac{t}{1.7}\right) + 0.2 \text{ rad} \\
\theta &= 0.1\sin\left(2\pi\frac{t}{300}\right) + 0.05\sin\left(2\pi\frac{t}{1.7}\right) - 0.4 \text{ rad} \\
\phi &= 0.1\sin\left(2\pi\frac{t}{300}\right) + 0.05\sin\left(2\pi\frac{t}{0.85}\right) + 0.5 \text{ rad}
\end{aligned}
\tag{27}
$$

One should notice that this trajectory and angular movement yield in a fully observable system [35], [37], [38].

REFERENCES

[1] R. Olfati-Saber, "Distributed Kalman filtering for sensor networks," in *46th IEEE Conference on Decision and Control*, New Orleans, Louisiana, USA, 2007, pp. 5492–5498.

[2] F. S. Cativelli, C. G. Lopes, and A. H. Sayed, "Diffusion strategies for distributed Kalman filtering: formulation and performance analysis," in *ARP Workshop on Cognitive Information Processing, 2008*. Santorini, Greece: ARP Workshop on Cognitive Information Processing, 2008.

[3] N. A. Carlson, "Federated filter for fault-tolerant integrated navigation systems," in *IEEE Position, Location and Navigation Symposium, 1988*, Orlando, Florida, USA, 1988, pp. 110–119.

[4] S. C. Felter, "An overview of decentralized Kalman filter techniques," in *IEEE Southern Tier Technical Conference, 1990*, 1990, pp. 79–87.

[5] H. Z. Qui, H. Y. Zhang, and H. Jin, "Fusion algorithm of correlated local estimates," *Aerospace Science and Technology*, vol. 8, pp. 619–629, 2004.

[6] F. Borreli, T. Keviczky, and J. G. Balas, "Collision-free uav formation flight using decentralized optimization and invariant sets," in *43th IEEE Conference on Decision and Control*, Atlantis, Paradise Island, Bahamas, 2004.

[7] P. Fergunson, T. Yang, M. Tillerson, and J. How, "New formation flying testbed for analyzing distributed estimation and control architectures," in *AIAA Guidance, Navigation and Control Conference, 2002*, 2002.

[8] P. Fergunson and J. How, "Decentralized estimation algorithms for formation flying spacecraft," in *AIAA Guidance, Navigation and Control Conference, 2003*, 2003.

[9] R. S. Smith and F. Y. Hadaegh, "Parallel estimation and control architectures for deep-space formation flying spacecraft," in *IEEE Aerospace Conference, 2006*. Santa Barbara, California, USA: IEEE Aerospace Conference, 2006.

[10] ——, "A distributed parallel estimation architecture for cooperative vehicle formation control," in *IEEE Aerospace Conference, 2006*. Minneapolis, Minnesota, USA: IEEE Aerospace Conference, 2006.

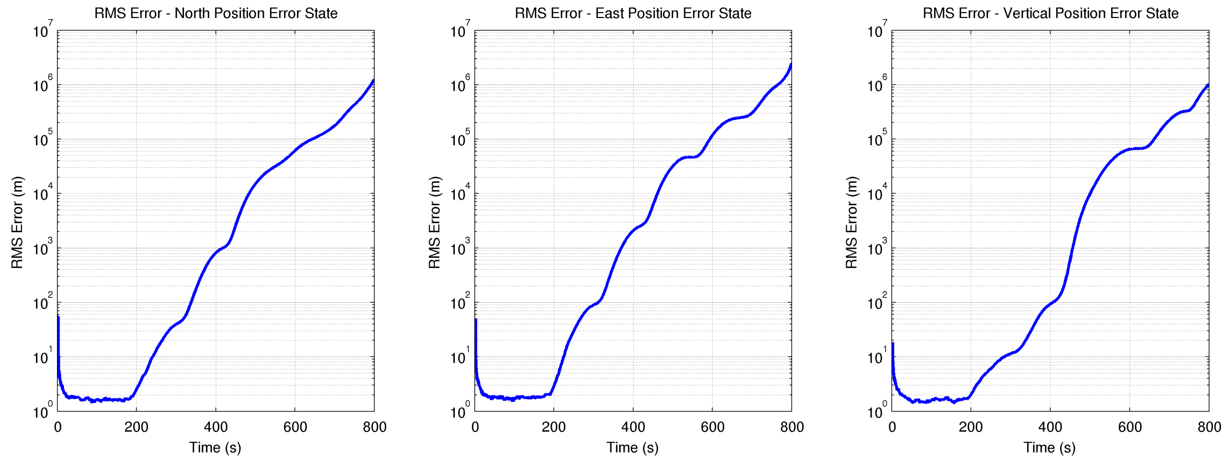

Fig. 2. Scenario 01: Delayed measurements naïvely fused - RMS errors of the position error components from 100 realizations.

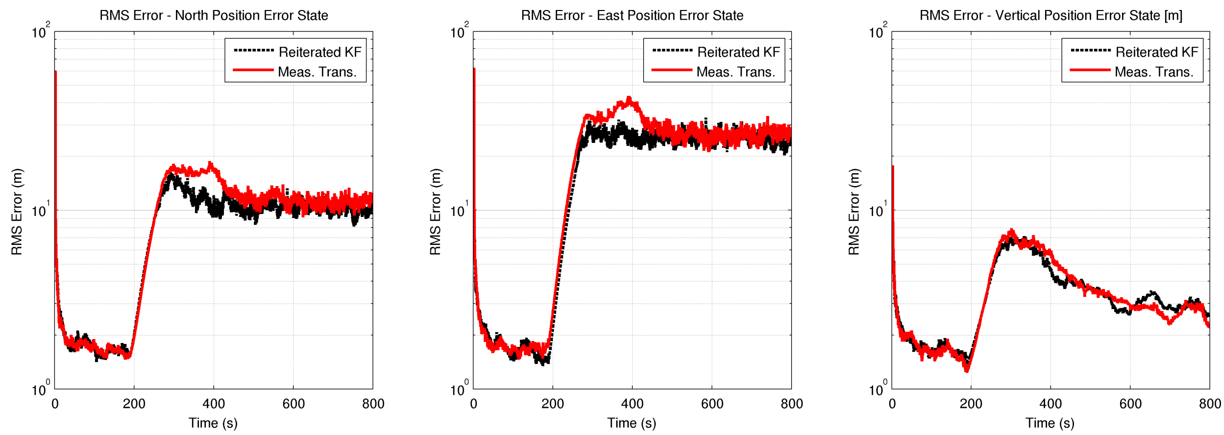

Fig. 3. Scenario 02: Delayed measurements correctly fused - RMS errors of the position error components from 100 realizations.

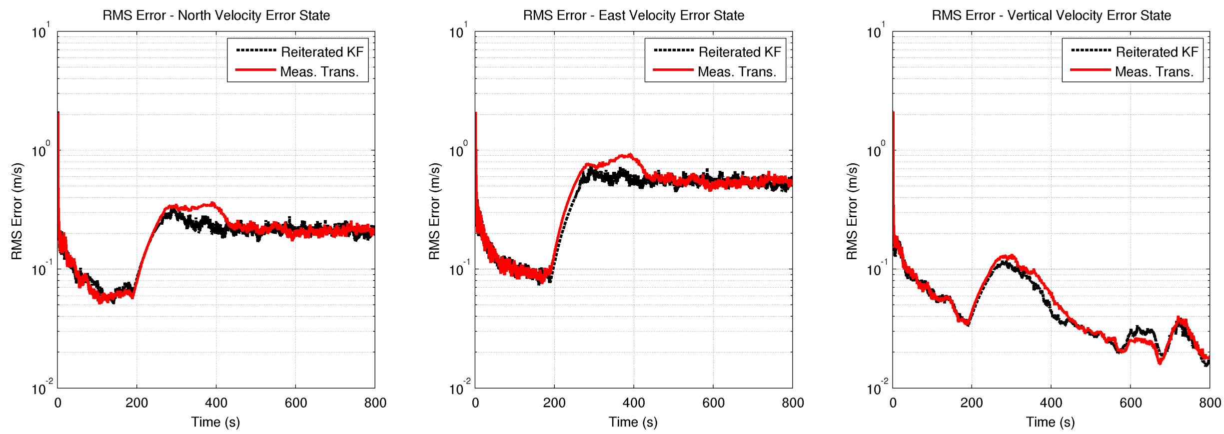

Fig. 4. Scenario 02: Delayed measurements correctly fused - RMS errors of the velocity error components from 100 realizations.

[11] S. M. Azizi and K. Khorasani, "A distributed Kalman filter for actuator fault estimation of deep space formation flying satellites," in *3th Annual IEEE International Systems Conference*, Vancouver, Canada, 2009.

[12] A. T. Alouani, "Linear distributed estimation," in *IEEE American Control Conference, 1987*, Minneapolis, United States of America, 1987.

[13] H. F. D.-W. M. T. Berg, "Generalized decentralized Kalman filters," in *IEEE American Control Conference, 1994*, Baltimore, Maryland, USA, 1994.

[14] D. K. Tasoulis, N. M. Adams, and D. J. Hand, "Selective fusion of out-of-sequence measurements," *Information Fusion*, vol. 11, no. 2, pp. 183–191, 2010.

[15] A. Matveev and A. Savkin, "The problem of state estimation via asynchronous communication channels with irregular transmission times," *IEEE Transactions on Automatic Control*, vol. 48, no. 4, pp. 670–676, 2003.

[16] K. Zhang, X. R. Li, and Y. Zhu, "Optimal update with out-of-sequence measurements," *IEEE Transactions on Signal Processing*, vol. 56, no. 6, pp. 1992–2004, 2005.

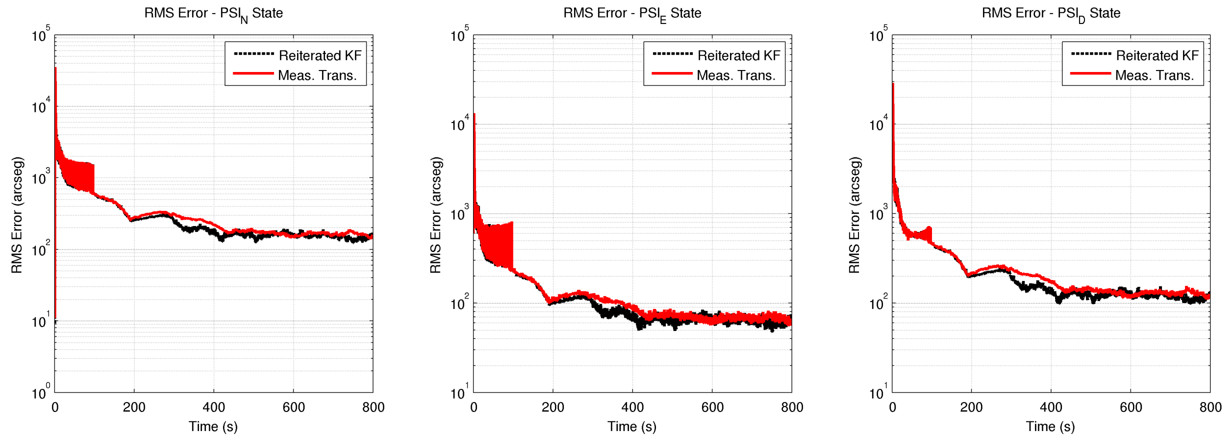

Fig. 5. Scenario 02: Delayed measurements correctly fused - RMS errors of the misalignment error components from 100 realizations.

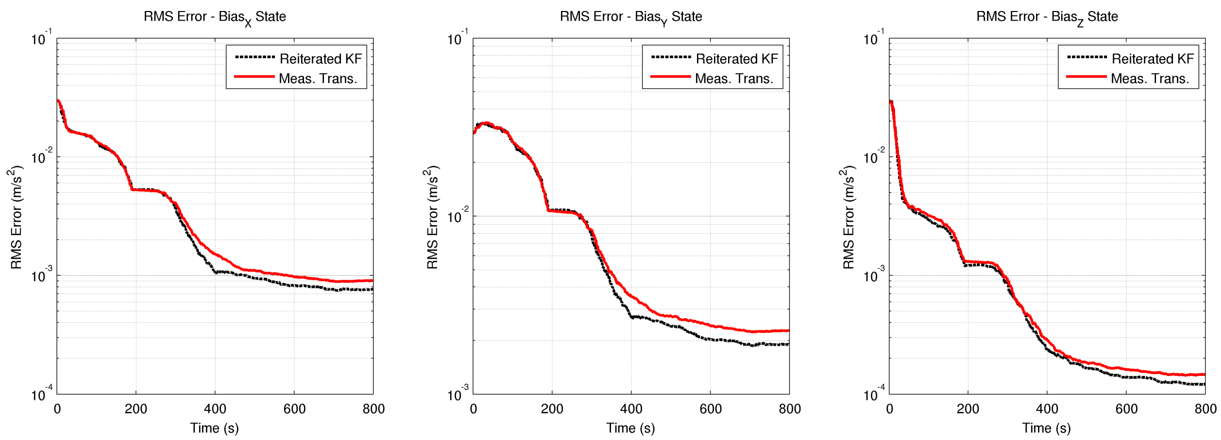

Fig. 6. Scenario 02: Delayed measurements correctly fused - RMS errors of the accelerometer bias components from 100 realizations.

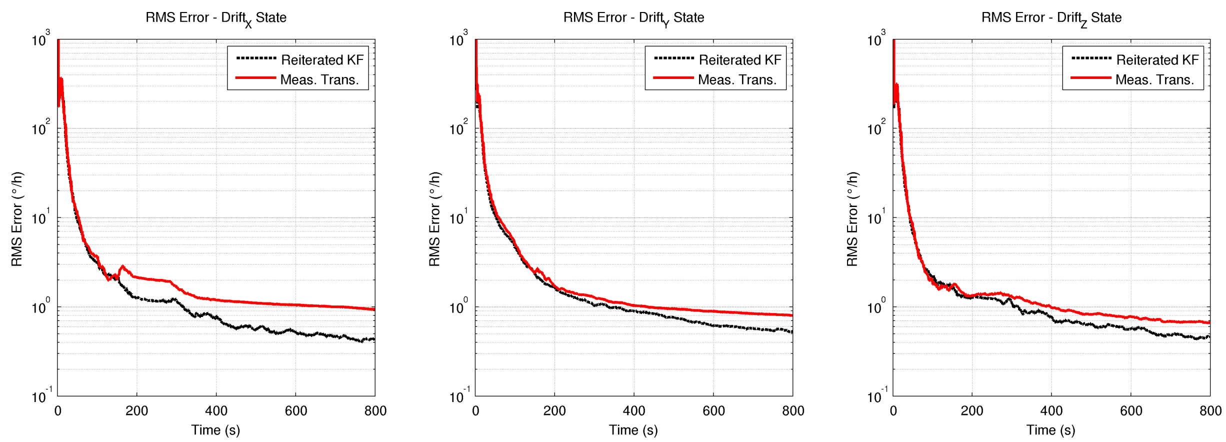

Fig. 7. Scenario 02: Delayed measurements correctly fused - RMS errors of the rate-gryo drift components from 100 realizations.

[17] X. Lu, H. Zhang, W. Wang, and K. Teo, "Kalman filtering for multiple time-delay systems," *Automatica*, vol. 41, no. 8, pp. 1455–1461, 2006.

[18] H. L. Alexander, "State estimation for distributed systems with sensing delay," in *Data structures and target classification*, V. Libby, Ed. SPIE, 1991, vol. 1470, pp. 103–111.

[19] T. D. Larsen, N. A. Andersen, O. Ravn, and N. K. Poulsen, "Incorporation of time delayed measurements in a discrete-time kalman filter," in *37th IEEE Conference on Decision and Control*, Florida, USA, 1998, pp. 3972–3977.

[20] E. Besada-Portas, J. A. Lopez-Orozco, J. A. Besada, and J. M. de la Cruz, "Multisensor out of sequence data fusion for estimating the state of discrete control systems," *IEEE Transactions on Automatic Control*, vol. 54, no. 7, pp. 1728–1732, 2009.

[21] R. G. Brown and G. L. Hartman, "Kalman filter with delayed states as observables," in *National Electronics Conference, 1968*, Chicago, IL, USA, 1968.

[22] Y. Bar-Shalom, M. Mallick, H. Chen, and R. Washburn, "One-step solution for the general out-of-sequence measurement problem in tracking," in *IEEE Aerospace Conference, 2002*, Montana, USA, 2002.

[23] A. Gopolakrishnan, N. S. Kaisare, and S. Narasimhan, "Incorporating

delayed and infrequent measurements in Extended Kalman filter based nonlinear state estimation," *Journal of Process Control*, vol. 21, pp. 119–129, 2011.
[24] K. Y. K. Leung, T. D. Barfoot, and H. H. T. Liu, "Decentralized localization of sparsely-communicating robot networks: A cetralized-equivalent approach," *IEEE Transactions on Robotics*, vol. 26, no. 1, pp. 62–77, 2010.
[25] S. Thomopoulos and L. Zhang, "Decentralized filtering with random sampling and delay," *Information Fusion*, vol. 81, no. 1-2, pp. 117–131, 1994.
[26] P. S. Maybeck, *Stochastic Models, Estimation and Control*. New York, United States of America: Academic Press, 1979, vol. 1.
[27] R. A. J. Chagas, "Distributed estimation of aided INS errors," Ph.D. dissertation, Instituto Tecnológico de Aeronáutica, soon to be defended.
[28] B. D. O. Anderson and J. B. Moore, *Optimal Filtering*. Englewood Cliffs, New Jersey, United States of America: Prentice-Hall, Inc., 1979.
[29] R. G. Brown and P. Y. C. Hwang, *Introduction to Random Signals and Applied Kalman Filtering*. United States of America: John Wiley & Sons, Inc., 1997.
[30] M. Vanvalkenburg. (2012, Apr) The matrix exponential function. [Online]. Available: http://math.berkeley.edu/%7Emjv/H54Lec22.pdf
[31] A. Weinred and I. Y. Bar-Itzhack, "The psi-angle error equation in strapdown inertial navigation systems," *IEEE Transactions on Aerospace and Electronic Systems*, vol. 14, no. 3, pp. 539–542, 1979.
[32] J. Lee, C. G. Park, and H. W. Park, "Multiposition alignment of strapdown inertial navigation system," *IEEE Transactions on Aerospace and Electronic Systems*, vol. 29, no. 4, pp. 1323–1328, 1993.
[33] J. Lapid-Maoz and I. Y. Bar-Itzhack, "Relative-location determination of cooperating aircraft," in *AIAA Guidance, Navigation and Control Conference, 2000*, Denver, CO, USA, 2000.
[34] O. Salychev, *Applied Inertial Navigation:Problems and Solutions*. Moscow, Russia: BMSTU Press, 2004.
[35] R. A. J. Chagas and J. Waldmann, "Geometric inference-based observability analysis digest of INS error model with GPS/magnetometer/camera aiding," in *19th Saint Petersburg International Conference on Integrated Navigation Systems*, Saint Petersburg, Russia, 2012.
[36] M. Shuster and S. Oh, "Three-axis attitude determination from vector observations," *Journal of Guidance, Control, and Dynamics*, vol. 4, no. 1, pp. 70–77, 1981.
[37] D. Goshen-Meskin and I. Y. Bar-Itzhack, "Observability analysis of piece-wise constant systems. ii. application to inertial navigation in-flight alignment [military applications]," *IEEE Transactions on Aerospace and Electronic Systems*, vol. 28, no. 4, pp. 1068–1075, oct 1992.
[38] D. Chung, C. G. Park, and J. G. Lee, "Observability analysis of strapdown inertial navigation system using Lyapunov transformation," in *35th IEEE Conference on Decision and Control*, Kobe, Japan, 1995, pp. 23–28.